Lysophosphatidic acid precursor levels decrease and an arachidonic acid-containing phosphatidylcholine level increases in the dorsal root ganglion of mice after peripheral nerve injury

メタデータ	言語: eng 出版者: Elsevier Scientific Publishers Ireland 公開日: 2019-12-06 キーワード (Ja): キーワード (En): 作成者: 三原, 唯暉 メールアドレス: 所属:
URL	http://hdl.handle.net/10271/00003671

This work is licensed under a Creative Commons Attribution-NonCommercial-ShareAlike 3.0 International License.

Neuroscience Letters 698 (2019) 69–75

Contents lists available at ScienceDirect

Neuroscience Letters

journal homepage: www.elsevier.com/locate/neulet

Research article

Lysophosphatidic acid precursor levels decrease and an arachidonic acid-containing phosphatidylcholine level increases in the dorsal root ganglion of mice after peripheral nerve injury

Yuki Mihara[a], Makoto Horikawa[b], Shumpei Sato[b], Fumihiro Eto[b,f], Mitsuru Hanada[a], Tomohiro Banno[a], Hideyuki Arima[a], Hiroki Ushirozako[a], Tomohiro Yamada[a], Dongmin Xu[a], Ayako Okamoto[a], Fumiyoshi Yamazaki[b], Shiro Takei[b,c], Takao Omura[a], Ikuko Yao[f], Yukihiro Matsuyama[a], Mitsutoshi Setou[b,d,e,*]

[a] Department of Orthopedic Surgery, Hamamatsu University School of Medicine, 1-20-1, Handayama, Higashi-ku, Hamamatsu, Shizuoka, 431-3192, Japan
[b] International Mass Imaging Center and Department of Cellular and Molecular Anatomy, Hamamatsu University School of Medicine, 1-20-1 Handayama, Higashi-ku, Hamamatsu, Shizuoka, 431-3192, Japan
[c] Department of Environmental Biology, College of Bioscience and Biotechnology, Chubu University, 1200 Matsumoto-cho, Kasugai, Aichi, 487-8501, Japan
[d] Preeminent Medical Photonics Education & Research Center, 1-20-1 Handayama, Higashi-ku, Hamamatsu, Shizuoka, 431-3192, Japan
[e] Department of Anatomy, The University of Hong Kong, 6/F, William MW Mong Block 21 Sassoon Road, Pokfulam, Hong Kong SAR, China
[f] Department of Optical Imaging, Institute for Medical Photonics Research, Preeminent Medical Photonics Education & Research Center, Japan

ARTICLE INFO

Keywords:
Peripheral nerve injury
Neuropathic pain
Lysophosphatidic acid
Sciatic nerve transection
Matrix-assisted laser desorption ionization
Imaging mass spectrometry

ABSTRACT

In the current study, we aimed to analyze the lipid changes in the dorsal root ganglion (DRG) after sciatic nerve transection (SNT) using matrix-assisted laser desorption/ionization imaging mass spectrometry (MALDI-IMS). We found that the arachidonic acid-containing phosphatidylcholine (AA-PC), PC(16:0/20:4) largely increased, while PC(16:0/18:1), PC(18:0/18:1) and phosphatidic acid (PA)(36:2) levels largely decreased in the DRG following nerve injury. Previous studies show that the increase in PC(16:0/20:4) was associated with neuropathic pain and that decrease in PC(16:0/18:1), PC(18:0/18:1), and PA(36:2) were due to producing lysophosphatidic acid (LPA), an initiator for neuropathic pain. These results suggest that the lipid changes in DRG after SNT could be the result of changes for the cause of neuropathic pain. Thus, blocking of LPA could be potential for treatment of neuropathic pain.

1. Introduction

Peripheral nerve injury provokes changes in neuronal, electrophysiological and immunological interactions within the spinal cord and dorsal root ganglion. Therefore, numerous investigations has been performed to elucidate the molecular and proteomic change occurring in the spinal cord after nerve injury [13,20,27]. Dorsal root ganglion, which is directly connected from peripheral nerve has been extensively studied for the molecular changes occurring after nerve injury [8,12,14,26]. However, how the expression of lipids change after nerve injury remains unknown.

Lipids are the most abundant biomolecules in the nervous system [17,19,22]. Lipid molecules are involved in many cellular functions including regulation of the physical properties of the cellular membrane and those involved in neurotransmitter signaling [1]. In our previously studies, we have focused on analyzing changes in phosphatidylcholines (PCs) in the spinal cord after sciatic nerve transection (SNT), spinal cord injury in the presence and absence of IL6 inhibitor and in amyotrophic lateral sclerosis model mice using matrix-assisted laser desorption/ionization imaging mass spectrometry (MALDI-IMS) [3,4,11,28]. MALDI-IMS is a powerful and practical tool for lipid analysis [9,23].

As massive transcriptional changes occur after peripheral nerve injury [6], we hypothesized that the lipids within the DRG could also be differentially regulated after nerve injury. The purpose of this study was to investigate the change of lipids in the DRG after sciatic nerve transection using MALDI-IMS.

* Corresponding author at: International Mass Imaging Center and Department of Cellular and Molecular Anatomy, Hamamatsu University School of Medicine, 1-20-1 Handayama, Higashi-ku, Hamamatsu, Shizuoka, 431-3192, Japan.
E-mail address: setou@hama-med.ac.jp (M. Setou).

https://doi.org/10.1016/j.neulet.2018.12.035
Received 18 August 2018; Received in revised form 17 December 2018; Accepted 22 December 2018
Available online 26 December 2018
0304-3940/ © 2018 The Authors. Published by Elsevier B.V. This is an open access article under the CC BY-NC-ND license (http://creativecommons.org/licenses/BY-NC-ND/4.0/).

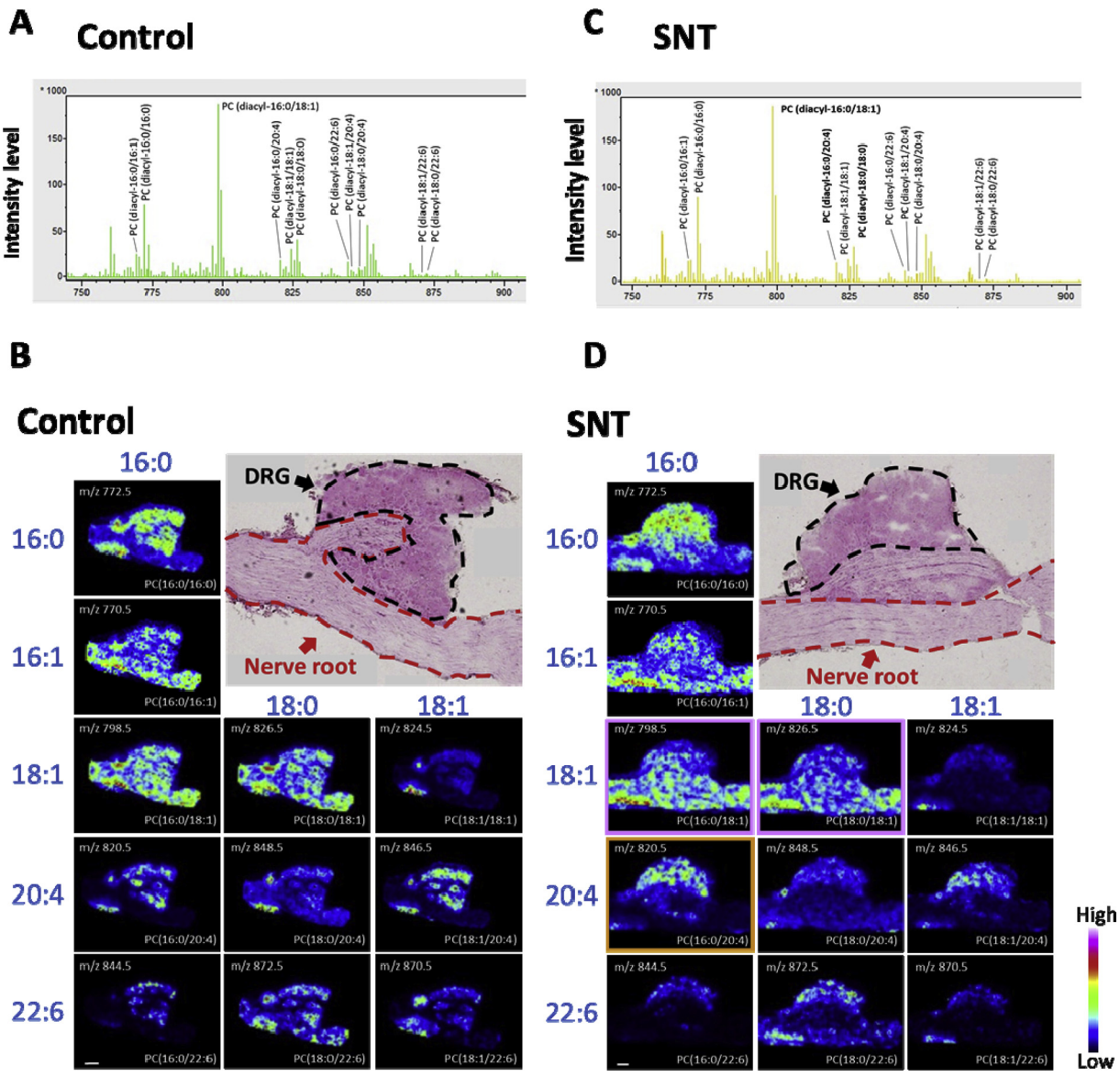

Fig. 1. Characterization of primary PC molecular species in DRG and nerve root of the control group.
A representative mass spectrum obtained from an entire control DRG and nerve root section by MALDI-IMS. In the spectrum, the intense mass peaks corresponding to 11 abundant PCs were assigned based on their masses and previously reported data [22] (A). Differential distribution of PC molecular species in a control DRG and nerve root section. An optical image of a hematoxylin and eosin-stained mouse DRG and nerve root section and ion images of PCs obtained from the consecutive section by MALDI-IMS are depicted. Ion images of PCs are arranged according to their fatty acid (FA) compositions; PCs with identical FA compositions at the sn-1 position are arranged lengthwise, while those with identical FA compositions at the sn-2 position are arranged horizontally [11] (B). The specific FA composition is associated with several unique localization features. In the DRG of the SNT mice, the signal intensity of PC(16:0/20:4) (*m/z* 820.5; enclosed in the orange frame), increased further and the signal intensities of PC(16:0/18:1) (*m/z* 798.5; enclosed in the pink frame) and PC(18:0/18:1) (*m/z* 826.5; enclosed in the pink frame) decreased further than those of control DRG (C, D). The detected ions were of potassium adducts. Scale bars: 200 μm.

2. Materials and methods

2.1. Animals

All experimental protocols were performed in accordance with the guidelines set by the Ethics Committee of Hamamatsu University School of Medicine. All experiments were conducted according to protocols approved by the Animal Care and Use Committee of the Hamamatsu University School of Medicine. Eight-week-old C57BL/6JJmsSlc male mice (weight: 16–21 g) purchased from SLC Inc. (Hamamatsu, Japan) were used in this study.

2.2. Chemicals

Methanol, potassium acetate, and ultrapure water were purchased from Wako Pure Chemical Industries (Osaka, Japan). Additionally 2,5-dihydroxybenzoic acid (DHB), a Matrix-Assisted Laser Desorption Ionization matrix, was purchased from Bruker Daltonics (Fremont, CA, USA). All chemicals used in this study were of the highest purity available.

2.3. Sciatic nerve transection model

Three mice were anesthetized with ketamine 100 mg/kg and xylazine 10 mg/kg. Sciatic nerve transection (SNT) was performed by transecting the left sciatic nerve at the mid-hind limb level. The skin

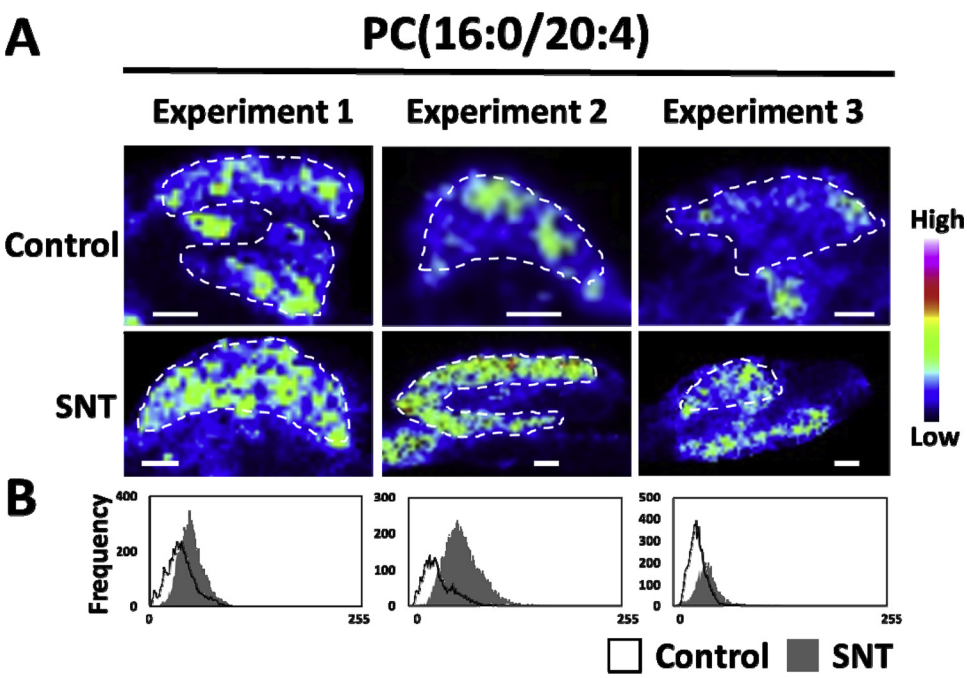

Fig. 2. Quantitative comparisons of AA-PC levels between control and SNT mice. This analysis was performed three times using one pair of mice, per experiment. The PC(16:0/20:4) (*m/z* 820.5) levels were increased in SNT mice (Fig. A and B). The signal intensities of these AA-PCs were higher in the DRG than in the nerve root (A). The detected ions were of potassium adducts. Scale bars: 200 µm. (B) The X and Y axes indicate gray level and frequency of pixel in image respectively.

layers were closed using a surgical stapler. Three mice were housed in a humidity- and temperature-controlled colony room with a 12 h light/dark cycle (lights on at 08:00) and food and water available ad libitum.

2.4. Tissue preparation for MALDI-IMS

Five days after SNT, the mice that had undergone SNT (SNT mice) were euthanized with a controlled overdose of pentobarbital sodium (25 mg/kg) and the L5 DRG were extracted and analyzed. Three naive mice were used as controls (control mice), and a total of 6 mice were used in this study. These DRG were embedded in carboxymethyl cellulose solution immediately after dissection and were flash frozen on dry ice and stored at −80 °C. Tissue sections (10 µm) were prepared at −20 °C using a cryostat (CM1950; Leica, Wetzler, Germany) and placed alternately onto glass slides coated with indium-tin-oxide (ITO) (Matsunami) for MALDI-IMS assessment, and onto un-coated glass slides (Matsunami) for hematoxylin and eosin staining. For MALDI-IMS analysis, a DRG section of one SNT mouse and that of one control were mounted onto the same ITO glass slide. These experiments were repeated three times.

2.5. IMS sample preparation and MALDI-IMS analysis

DHB solution (40 mg/mL DHB, 20 mM potassium acetate, 70% methanol) was used as the matrix solution. The matrix solution (approximately 1000 µl) was sprayed over the tissue surface using a TM-Sprayer (HTX Technologies; Carrboro, NC, USA). In the TM-Sprayer, a constant flow of heated sheath gas (N_2, set at 10 psi) was delivered conjointly with the matrix solution spray. The temperature of the sheath gas was maintained at 75 °C. The solvent pump system used was a Smartline P1000 (Knauer, Berlin, Germany) operated at a flow rate of 0.3 mL/min. The TM-Sprayer software was used for the system operations. Tissue sections were spray coated with the matrix solution so that extraction and co-crystallization could be performed simultaneously. MALDI-IMS analyses were performed using a MALDI-Fourier transform ion cyclotron resonance type instrument (Solarix XR; Bruker Daltonics) equipped with a Bruker Smartbeam-II™ Laser. The laser was set to the small spot size with 50% laser power. Mass spectra ranging from mass-to-charge ratio (*m/z*) 600 to 1000 were collected. The laser scan pitch was set to 25 µm. Calibration of the *m/z* values was performed for each MALDI-IMS measurement using a standard calibration substance, namely sodium formate. Signals were collected using flexControl software (Bruker Daltonics) and reconstruction of ion images (normalized by total ion current) was performed with flexImaging 4.0 software (Bruker Daltonics). To distinguish the nerve roots from the cell bodies, we performed HE staining on a consecutive section (Fig. S1). The difference of HE staining intensity helped us to clarify the borders of these two regions in IMS figures. In the figures, the borders are marked with lines. The same method was used in our previous study [28].

2.6. Immunohistochemistry

Frozen sections mounted on MAS-coated glass slides were equilibrated at room temperature for 10 min and then fixed with 2% paraformaldehyde for 15 min at room temperature. After washing three times with PBS for 5 min, sections were blocked with blocking solution [PBS containing 1% bovine serum albumin, 2% blocking reagent (Roche 11,096,176,001), and 0.1% Triton X-100] for 60 min at room temperature. Sections were incubated with the primary antibodies, rat anti-F4/80 (1:200; Abcam, Cambridge, United Kingdom) and rabbit anti-P2X purinoceptor 4 (P2RX4; 1:200; Proteintech), in a humidified chamber at 4 °C overnight, then washed three times with PBS, and incubated for 60 min at room temperature with the secondary antibodies Alexa Fluor 594 donkey anti-rat IgG (Abcam, Cambridge, United Kingdom) and Alexa Fluor 488 goat anti-rabbit IgG (Abcam, Cambridge, United Kingdom). Slides were mounted with VECTASHIELD Antifade Mounting Medium with DAPI (Vector Laboratories, Inc, Burlingame, USA). Images were collected using IX83 microscope (Olympus, Japan). Final adjustment of contrast and intensity was done using Adobe Photoshop.

2.7. Histogram analysis

Each lipid images taken by MALDI IMS analysis were expressed as gray scale using flexImagin 4.0 software (Bruker Daltonics). In the gray scale images, the peak intensities of each pixel were transformed to percentage and expressed as gray level. The gray scale images were imported to ImageJ (https://imagej.nih.gov/ij/) and then converted to 8-bit gray scale. Finally, histogram was generated from each region of interest (ROI) and that of pixel binned by 255 Gy level was depicted.

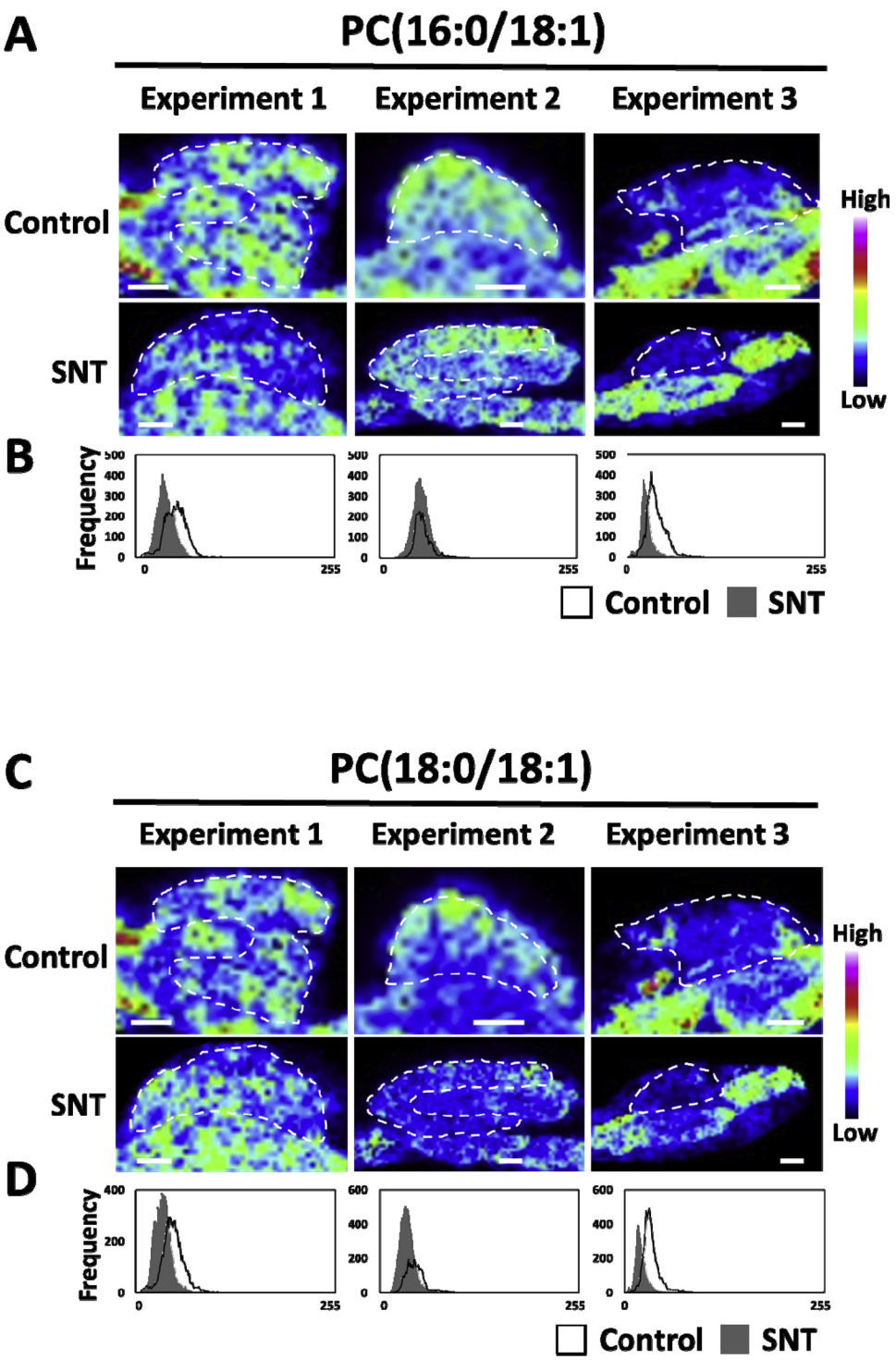

Fig. 3. Quantitative comparisons of MUFA-PC levels between control and SNT mice. This analysis was performed three times using one pair of mice, per experiment. PC(16:0/18:1) (*m/z* 798.5) and PC(18:0/18:1) (*m/z* 826.5) levels decreased in the DRG of the SNT mice (A–D). The signal intensities of PC(16:0/18:1) (*m/z* 798.5) and PC(18:0/18:1) (*m/z* 826.5) were evenly detected in the DRG and the nerve root (A, C). The detected ions were of potassium adducts. Scale bars: 200 μm. (B, D) The X and Y axes indicate gray level and frequency of pixel in image respectively.

The dynamic ranges of signal intensities were consistent in each experiment.

X-axis represents the relative signal intensities and Y-axis shows the amount of data points.

2.8. Statistical analysis

Cohen's method was used for evaluating the differences of the data [7]. We calculated Cohen's d of the gray level of pixels in image for 3 biological replicates. If the Cohen's d larger than 0.8 for increase or smaller than -0.8 for decrease in SNT compared with control sample and more than 2 biological replicates pass the criteria, we defined its lipid is largely changed by SNT. Mean value, Standard deviation (SD) and the results of statistical analysis of each specimen were summarized in Table S1. Welch's *t*-test was performed using the Statistical Package for the Social Science (SPSS) software (version 25; SPSS, Chicago, IL,

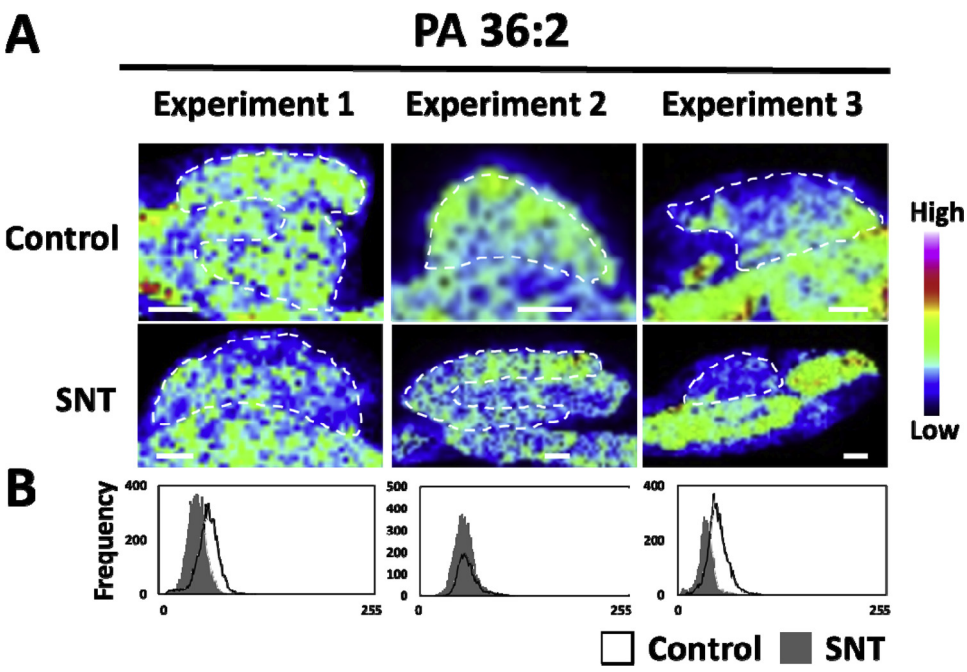

Fig. 4. Quantitative comparisons of PA levels between control and SNT mice. This analysis was performed three times using one pair of mice, per experiment. The PA(36:2) (*m/z* 739.5) level decreased in the DRG of SNT mice (A and B). The detected ions were of potassium adducts. Scale bars: 200 μm. (B) The X and Y axes indicate gray level and frequency of pixel in image respectively.

USA).

3. Results

3.1. MALDI-IMS analysis for the dorsal root ganglion and nerve root

First we analyzed the lipid distribution in the DRG and the nerve root in control mice using MALDI-IMS. Mass spectra ranging from *m/z* 600 to 1000 were collected and 11 phospholipids that were identified in the previous study [22] were analyzed (Fig. 1A). The detected ions were of potassium adducts. The signal intensities and distributions of the PCs are presented in Fig. 1B.

After nerve injury, of the signal intensity of PC(16:0/20:4) (*m/z* 820.5) became stronger and a the signal intensities of PC(16:0/18:1) (*m/z* 798.5) and PC(18:0/18:1) (*m/z* 826.5) appeared to be weaker (Fig. 1C, D).

3.2. Increased level of PC(16:0/20:4) in the DRG after nerve injury

In our previous study [28], we found increase of an arachidonic acid-containing PC (AA-PC), PC(16:0/20:4) (*m/z* 820.5), which is one of the n-6- polyunsaturated fatty acids (PUFAs), in the ipsilateral ventral and dorsal horns of the spinal cord after SNT. As with our previous study, the signal intensity of the AA-PC was largely higher in the DRG of the SNT mice in comparison to control mice (Fig. 2A, B). However, we observed no difference in the signal intensity of PC(18:0/20:4) (*m/z* 848.5) (A, B) and PC(18:1/20:4) (*m/z* 846.5) in comparison with the controls (Fig. S2 A–D).

3.3. No change in docosahexaenoic acid-containing PC levels in the DRG after nerve injury

Docosahexaenoic acid (DHA), one of the n-3 PUFAs, has been reported to be involved in neuronal protection in the injured hippocampus [10]. We therefore analyzed the distribution of DHA-containing PCs (DHA-PCs), such as PC(16:0/22:6) (*m/z* 844.5), PC(18:0/22:6) (*m/z* 872.5), and PC(18:1/22:6) (*m/z* 870.5), but the levels of these DHA-PCs did not change after SNT (Fig S3 A–F).

3.4. Decrease in levels of monounsaturated fatty acid -containing PCs in the DRG after nerve injury

Monounsaturated fatty acid (MUFA) is another class of fatty acid species and generally situated at the sn-2 position of several phospholipids [21]. MUFA-PCs, PC(16:0/18:1) (*m/z* 798.5) and PC(18:0/18:1) (*m/z* 826.5) were detected in both DRG and the nerve root (Fig. 3A, C). After nerve injury, there was a large decrease of both PC(16:0/18:1) and PC(18:0/18:1) in the DRG in comparison with the controls (Fig. 3A-D). However, we observed no difference in the signal intensity of PC(18:1/18:1) (*m/z* 824.5) in comparison with the controls (Fig. S4A, B).

3.5. Altered levels of PA in the DRG

Using the MALDI-IMS data, we performed an unbiased screening of the lipids that were present at different levels in the DRG after nerve injury (Fig. 4). We found that the phosphatidic acid (PA)(36:2) (*m/z* 739.5) level largely decreased in the DRG of SNT mice (Fig. 5A, B), but the PA (34:1) (*m/z* 713.5) and PA(36:1) (*m/z* 741.5) level remained unchanged (Fig. S5 A–D).

3.6. Increased intensities of F4/80 immuno-positive cells in the DRG after nerve injury

The staining showed marked increase of the F4/80 immuno-positive cells with nerve injury, resembling the expression pattern of PC(16:0/20/4) (Fig. 5A). P2 × 4 receptors in the spinal cord activate microglia, and correlate with generation of neuropathic pain [5]. We therefore pursued immunostaining of the P2RX4. However, there were no obvious P2RX4 immuno-positive cells change between control and SNT mice (Fig. 5B). There were no obvious co-localization between F4/80 and P2RX4 immuno-positive cells (Fig. 5C).

4. Discussion

In this study, we found that the PC (16:0/20:4) level significantly increased in the DRG following nerve injury as with our previous study showing large increase of PC (16:0/20:4) in the dorsal horn after peripheral nerve injury [28]. This could partly be due to the activated

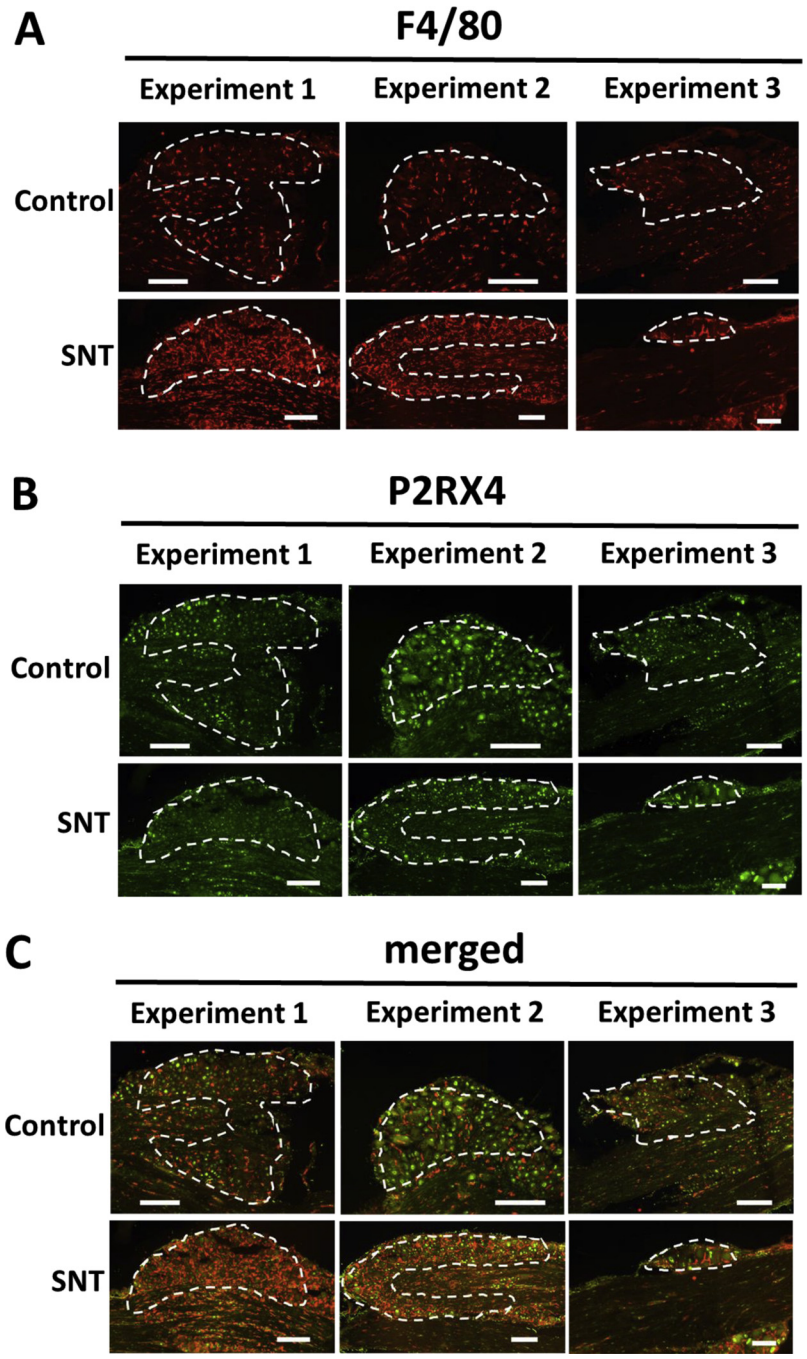

Fig. 5. Immunostaining of F4/80 and P2RX4 between control and SNT mice. The staining showed marked increase of the F4/80 immuno-positive cells with nerve injury (A). There were no obvious P2RX4 immuno-positive cells change between Control and SNT mice (B). The P2RX4 immuno-positive cells did not co-localize with F4/80 staining cells (C).

macrophages within the DRG as we observed marked increase of F4/80 immuno-positive cells.

We observed large signal reduction of PC(16:0/18:1) and PC(18:0/18:1) in the DRG after nerve injury. This decline is considered to be associated with production of lysophosphatidic acid (LPA) because LPA is generated from lysophosphatidylcholine (LPC) by autotaxin enzymes [24,25]. PC(16:0/18:1) and PC(18:0/18:1) are considered to be consumed to produce LPC. Indeed, the levels of 16:0-, 18:0-, and 18:1-LPC in the spinal cord and dorsal root increase after sciatic nerve injury [18]. Moreover, the levels of 16:0-, 18:0-, and 18:1-LPA in the spinal dorsal horn also increase after sciatic nerve injury [15]. In our unbiased screening of lipids in the DRG, PA(36:2) levels decreased largely after SNT. We also consider this reduction to be associated with the production of LPA because LPA is generated from PA by phospholipase A2 (PLA2) enzymes [2]. Therefore, we speculate that PA(36:2) have been consumed to produce LPA.

In conclusion, we observed increased AA-PC and decline in the precursors of LPA in the DRG 5 days after sciatic nerve injury. These lipid changes after nerve injury were considered to be correlated with neuropathic pain. LPA antagonist [13] and PLA2 inhibitor [16] is known to attenuate neuropathic pain in vivo. However, LPA has not yet been considered as a target for the treatment of neuropathic pain in clinical cases. This report suggested a potential role of LPA in the generation of pain within the DRG and could be a novel targeted for the treatment of neuropathic pain.

Conflicts of interest

The authors declare no conflict of interest.

Acknowledgements

This study was supported by MEXT/JSPS KAKENHI Grant Number JP26460388, Japan Agency for Medical Research and Development (AMED) under Grant Number JP16KT0134, Japan Science and Technology Agency (JST) Program for Creating STart-ups from Advanced Research and Technology (START) under Grant Number ST292006UT and Imaging Platform supported by the Ministry of Education, Culture, Sports, Science and Technology (MEXT), Japan. We also would like to thank Dr. T. Ojima for giving advice to statistical analysis.

Appendix A. Supplementary data

Supplementary material related to this article can be found, in the online version, at doi:https://doi.org/10.1016/j.neulet.2018.12.035.

References

[1] J.A. Allen, R.A. Halverson-Tamboli, M.M. Rasenick, Lipid raft microdomains and neurotransmitter signalling, Nat. Rev. Neurosci. 8 (2007) 128–140.
[2] J. Aoki, A. Taira, Y. Takanezawa, Y. Kishi, K. Hama, T. Kishimoto, K. Mizuno, K. Saku, R. Taguchi, H. Arai, Serum lysophosphatidic acid is produced through diverse phospholipase pathways, J. Biol. Chem. 277 (2002) 48737–48744.
[3] H. Arima, M. Hanada, T. Hayasaka, N. Masaki, T. Omura, D. Xu, T. Hasegawa, D. Togawa, Y. Yamato, S. Kobayashi, T. Yasuda, Y. Matsuyama, M. Setou, Blockade of IL-6 signaling by MR16-1 inhibits reduction of docosahexaenoic acid-containing phosphatidylcholine levels in a mouse model of spinal cord injury, Neuroscience 269 (2014) 1–10.
[4] H. Arima, T. Omura, T. Hayasaka, N. Masaki, M. Hanada, D. Xu, T. Banno, K. Kobayashi, H. Takeuchi, K. Kadomatsu, Y. Matsuyama, M. Setou, Reductions of docosahexaenoic acid-containing phosphatidylcholine levels in the anterior horn of an ALS mouse model, Neuroscience 297 (2015) 127–136.
[5] T. Banno, T. Omura, N. Masaki, H. Arima, D. Xu, A. Okamoto, M. Costigan, A. Latremoliere, Y. Matsuyama, M. Setou, Arachidonic acid containing phosphatidylcholine increases due to microglial activation in ipsilateral spinal dorsal horn following spared sciatic nerve injury, PLoS One 12 (2017) e0177595.
[6] V. Chandran, G. Coppola, H. Nawabi, T. Omura, R. Versano, E.A. Huebner, A. Zhang, M. Costigan, A. Yekkirala, L. Barrett, A. Blesch, I. Michaelevski, J. Davis-Turak, F. Gao, P. Langfelder, S. Horvath, Z. He, L. Benowitz, M. Fainzilber, M. Tuszynski, C.J. Woolf, D.H. Geschwind, A systems-level analysis of the peripheral nerve intrinsic axonal growth program, Neuron 89 (2016) 956–970.
[7] J. Cohen, A power primer, Psychol. Bull. 112 (1992) 155–159.
[8] M. Costigan, K. Befort, L. Karchewski, R.S. Griffin, D. D'Urso, A. Allchorne, J. Sitarski, J.W. Mannion, R.E. Pratt, C.J. Woolf, Replicate high-density rat genome oligonucleotide microarrays reveal hundreds of regulated genes in the dorsal root ganglion after peripheral nerve injury, BMC Neurosci. 3 (2002) 16.
[9] S.R. Ellis, M.R.L. Paine, G.B. Eijkel, J.K. Pauling, P. Husen, M.W. Jervelund, M. Hermansson, C.S. Ejsing, R.M.A. Heeren, Automated, parallel mass spectrometry imaging and structural identification of lipids, Nat. Methods (2018).
[10] C. Garcia-Caceres, M.H. Tschop, Hypothalamic Injury: Fish Oil to the Rescue!, Diabetes 65 (2016) 551–553.
[11] M. Hanada, Y. Sugiura, R. Shinjo, N. Masaki, S. Imagama, N. Ishiguro, Y. Matsuyama, M. Setou, Spatiotemporal alteration of phospholipids and prostaglandins in a rat model of spinal cord injury, Anal. Bioanal. Chem. 403 (2012) 1873–1884.
[12] S. Li, C. Xue, Y. Yuan, R. Zhang, Y. Wang, B. Yu, J. Liu, F. Ding, Y. Yang, X. Gu, The transcriptional landscape of dorsal root ganglia after sciatic nerve transection, Sci. Rep. 5 (2015) 16888.
[13] R.P. Lindblom, A. Berg, M. Strom, S. Aeinehband, C.A. Dominguez, F. Al Nimer, N. Abdelmagid, M. Heinig, J. Zelano, K. Harnesk, N. Hubner, B. Nilsson, K.N. Ekdahl, M. Diez, S. Cullheim, F. Piehl, Complement receptor 2 is up regulated in the spinal cord following nerve root injury and modulates the spinal cord response, J. Neuroinflammation 12 (2015) 192.
[14] J.A. Lindborg, J.P. Niemi, M.A. Howarth, K.W. Liu, C.Z. Moore, D. Mahajan, R.E. Zigmond, Molecular and cellular identification of the immune response in peripheral ganglia following nerve injury, J. Neuroinflammation 15 (2018) 192.
[15] L. Ma, J. Nagai, J. Chun, H. Ueda, An LPA species (18:1 LPA) plays key roles in the self-amplification of spinal LPA production in the peripheral neuropathic pain model, Mol. Pain 9 (2013) 29.
[16] L. Ma, H. Uchida, J. Nagai, M. Inoue, J. Aoki, H. Ueda, Evidence for de novo synthesis of lysophosphatidic acid in the spinal cord through phospholipase A2 and autotaxin in nerve injury-induced neuropathic pain, J. Pharmacol. Exp. Ther. 333 (2010) 540–546.
[17] S. Mikawa, M. Suzuki, C. Fujimoto, K. Sato, Imaging of phosphatidylcholines in the adult rat brain using MALDI-TOF MS, Neurosci. Lett. 451 (2009) 45–49.
[18] J. Nagai, H. Ueda, Pre-emptive morphine treatment abolishes nerve injury-induced lysophospholipid synthesis in mass spectrometrical analysis, J. Neurochem. 118 (2011) 256–265.
[19] D. Piomelli, G. Astarita, R. Rapaka, A neuroscientist's guide to lipidomics, Nature reviews, Neuroscience 8 (2007) 743–754.
[20] T. Scheid, L.D. Bosco, R.P. Guedes, M.A. Pavanato, A. Bello-Klein, W.A. Partata, Sciatic nerve transection modulates oxidative parameters in spinal and supraspinal regions, Neurochem. Res. 38 (2013) 935–942.
[21] A.D. Southam, F.L. Khanim, R.E. Hayden, J.K. Constantinou, K.M. Koczula, R.H. Michell, M.R. Viant, M.T. Drayson, C.M. Bunce, Drug redeployment to kill leukemia and lymphoma cells by disrupting SCD1-Mediated synthesis of monounsaturated fatty acids, Cancer Res. 75 (2015) 2530–2540.
[22] Y. Sugiura, Y. Konishi, N. Zaima, S. Kajihara, H. Nakanishi, R. Taguchi, M. Setou, Visualization of the cell-selective distribution of PUFA-containing phosphatidylcholines in mouse brain by imaging mass spectrometry, J. Lipid Res. 50 (2009) 1776–1788.
[23] Y. Sugiura, M. Setou, Imaging mass spectrometry for visualization of drug and endogenous metabolite distribution: toward in situ pharmacometabolomes, J. Neuroimmune Pharmacol. 5 (2010) 31–43.
[24] A. Tokumura, E. Majima, Y. Kariya, K. Tominaga, K. Kogure, K. Yasuda, K. Fukuzawa, Identification of human plasma lysophospholipase D, a lysophosphatidic acid-producing enzyme, as autotaxin, a multifunctional phosphodiesterase, J. Biol. Chem. 277 (2002) 39436–39442.
[25] M. Umezu-Goto, Y. Kishi, A. Taira, K. Hama, N. Dohmae, K. Takio, T. Yamori, G.B. Mills, K. Inoue, J. Aoki, H. Arai, Autotaxin has lysophospholipase D activity leading to tumor cell growth and motility by lysophosphatidic acid production, J. Cell Biol. 158 (2002) 227–233.
[26] V. Vigneswara, M. Berry, A. Logan, Z. Ahmed, Caspase-2 is upregulated after sciatic nerve transection and its inhibition protects dorsal root ganglion neurons from apoptosis after serum withdrawal, PLoS One 8 (2013) e57861.
[27] S. Wakisaka, K.C. Kajander, G.J. Bennett, Increased neuropeptide Y (NPY)-like immunoreactivity in rat sensory neurons following peripheral axotomy, Neurosci. Lett. 124 (1991) 200–203.
[28] D. Xu, T. Omura, N. Masaki, H. Arima, T. Banno, A. Okamoto, M. Hanada, S. Takei, S. Matsushita, E. Sugiyama, M. Setou, Y. Matsuyama, Increased arachidonic acid-containing phosphatidylcholine is associated with reactive microglia and astrocytes in the spinal cord after peripheral nerve injury, Sci. Rep. 6 (2016) 26427.